The electrical conductivity of expanded liquid caesium

1992 J. Phys.: Condens. Matter 4 1659

(http://iopscience.iop.org/0953-8984/4/7/005)

J. Phys.: Condens. Matter 4 (1992) 1659–1669. Printed in the UK

The electrical conductivity of expanded liquid caesium

R Redmer†, H Reinholz†, G Röpke†, R Winter‡, F Noll‡ and F Hensel‡

† Universität Rostock, Fachbereich Physik, Universitätsplatz 3, D-2500 Rostock, Federal Republic of Germany

‡ Philipps-Universität Marburg, Fachbereich Physikalische Chemie, Hans Meerwein Strasse, D-3550 Marburg, Federal Republic of Germany

Received 30 August 1991

Abstract. Recently it has been shown that the nearly free electron model for describing the electrical, magnetic and optical properties of expanded liquid caesium has already broken down by the time three times the critical density is reached, i.e. long before the transition from the metallic to the non-metallic state occurs, which seems to coincide with the critical point of the liquid–vapour phase transition ($T_c = 1924$ K, $p_c = 92$ bar, $\rho_c = 0.38$ g cm^{-3}). We discuss the deviations from the nearly free electron model within the framework of a consistent quantum statistical approach to the electrical conductivity, which leads to a generalized Ziman formula, taking into account electron–electron scattering, arbitrary degeneracy and screening. Further possible mechanisms that might contribute to the behaviour of the electrical conductivity, such as the formation of bound states, are also discussed.

1. Introduction

Over the last few years, considerable effort has been put into investigating the structural, thermodynamic, electrical and magnetic properties of liquid alkali metals expanded by heating towards their liquid–vapour critical points (for a review, see e.g. [1]). Measurements of the liquid–vapour coexistence curve, the electrical conductivity, the static magnetic susceptibility and the Knight shift of expanded liquid caesium have indicated that a metal–non-metal transition occurs near the critical point of the liquid–vapour phase transition. This implies that the interatomic forces must exhibit drastic changes as the density of the fluid is decreased towards the critical value.

Recently, Winter *et al* [2, 3] determined the static structure factor $S(Q)$ and the pair correlation function $g(R)$ of fluid caesium over wide ranges of temperature and pressure by neutron diffraction experiments. They found that the dominant effect on the physical properties during the expansion derives from a reduced average coordination number N_1 rather than from an increased next-neighbour distance R_1.

Measurements of the electrical DC conductivity [4] have shown that the metallic properties of the fluid phase are lost at conditions close to the critical point and that the metal–non-metal transition probably coincides with the liquid–vapour critical point (see

0953-8984/92/071659 + 11 $04.50

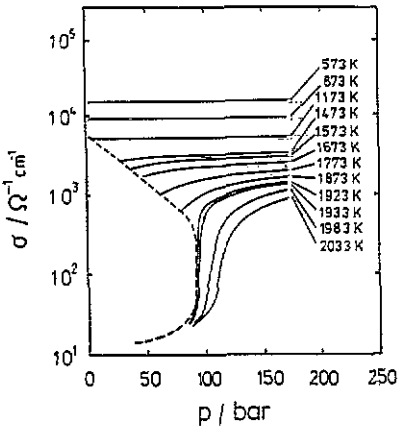

Figure 1. The electrical conductivity σ of caesium as a function of pressure and temperature [4].

figure 1; $T_c = 1924$ K, $p_c = 92$ bar, $\rho_c = 0.38$ g cm^{-3} [5]). By correlating the structural and electrical conductivity data with known equation of state data, further information about the electrical transport in expanded fluid metals can be gained. In particular, the comparison with the standard theoretical approach to the electrical properties of liquid metals, the Ziman–Faber theory, exhibits the limiting validity of the nearly free electron model.

A general theoretical treatment of fluid metals at low densities is still lacking but there is a close connection to the behaviour of dense and low-temperature plasmas which are continuously following the density–temperature domain of expanded fluids in the supercritical region. We will present a consistent quantum statistical approach which has been successfully applied for calculating the transport properties of non-degenerate, partially ionized hydrogen and alkali plasmas [6–13]. However, it is also valid for describing the electronic transport in degenerate electron systems such as the expanded fluid metals. We studied the influence of different mechanisms in order to explain the deviations observed between the experimental values for the electrical conductivity and the standard Ziman–Faber theory at lower densities.

2. The electrical conductivity

The electrical conductivity of Coulomb systems is known in the limiting cases of non-degenerate low-density plasmas (Spitzer formula [14]), and highly degenerate liquid metals (Ziman formula [15]). Since the conductivity governed by the Coulomb interaction is a universal function of the temperature and density, a consistent quantum statistical approach to the transport coefficients should be valid for arbitrary degeneracy.

The formation of such a general approach to the transport coefficients is possible within the frame of linear response theory, given here in an extended version originally developed by Zubarev [16] for mechanical and non-mechanical perturbations of an open system. The starting point is the Liouville–von Neumann equation for the non-equilibrium statistical operator ρ which determines the time-dependent mean values of arbitrary operators $\langle A \rangle^t = \mathrm{Tr}\{\rho(t)A\}$.

$$(\partial/\partial t)\rho(t) + (\mathrm{i}/\hbar)[H(t), \rho(t)] = 0 \tag{1a}$$

$$H = H_S + H_F \qquad H_F = -E\sum_i e_i r_i^z \equiv -\boldsymbol{E}\cdot\boldsymbol{R} \tag{1b}$$

$$H_S = \sum_c \sum_k E_c(k) a_c^+(k) a_c(k) + \tfrac{1}{2}\sum_{c,d}\sum_{kpq} e_c e_d V(q) a_c^+(k+q) a_d^+(p-q) a_d(p) a_c(k).$$

H is the Hamilton operator for an electron–ion system with an external electric field E, $E_c(k) = \hbar^2 k^2/2m_c$ denotes the kinetic energy of particles of species c = e, i and $V(q) = 4\pi/q^2$ is the Coulomb interaction. $a_c^+(k)$ and $a_c(k)$ are the creation and annihilation operators, respectively, for a particle in the state $|k\rangle$, here k denotes the spin and wave number vector, and e_c is the electrical charge of particles of species c.

Equation (1*a*) has to be modified in order to account for the time irreversibility of the evolution of the system. Besides the projection operator method [17] for the construction of a so-called 'relevant' statistical operator $\rho_{rel}(t)$, the definition of a generalized Gibbs state as the relevant statistical operator was employed by Robertson [18], and later by Zubarev [16], for the derivation of a general, irreversible equation of motion. Within this method, the relevant statistical operator

$$\rho_{rel} = \frac{1}{Z_{rel}} \exp\left(-\beta(H_S - \mu N) + \beta\sum_\nu F_\nu(t) B_\nu\right) \tag{2}$$

(where μ is the chemical potential, N is the particle number, and $\beta = 1/k_B T$) is determined from the maximum of entropy $S(t) = -k_B \operatorname{Tr}\{\rho_{rel}(t) \ln \rho_{rel}(t)\}$ at given mean values $\langle B_\nu\rangle^t$ of a set of relevant observables $\{B_\nu\}$. These quantities characterize the non-equilibrium state and fulfil the subsidiary conditions

$$\langle B_\nu\rangle^t = \operatorname{Tr}\{\rho(t) B_\nu\} \equiv \operatorname{Tr}\{\rho_{rel}(t) B_\nu\} \tag{3}$$

which simultaneously fix the thermodynamic parameters $F_\nu(t)$. In the case of thermodynamic equilibrium, no further relevant observables are needed and $\{B_\nu\} = 0$. This corresponds to the Kubo method.

However, the relevant statistical operator (2) is not a solution of the Liouville–von Neumann equation (1*a*) but it can be employed to define the correct initial conditions for solving it. Assuming the principle of weakening of initial correlations [19], and with reference to Abel's theorem [20], the following equation of motion can be derived for the non-equilibrium statistical operator:

$$\frac{\partial}{\partial t}\rho(t) + \frac{\mathrm{i}}{\hbar}[H(t), \rho(t)] = \lim_{\varepsilon\to 0} \varepsilon[\rho(t) - \rho_{rel}(t)]. \tag{4}$$

The limit $\varepsilon \to +0$ has to be taken after the thermodynamic limit. Finally, the general solution of (4) can be given after integrating by parts,

$$\rho(t) = \rho_{rel}(t) - \lim_{\varepsilon\to 0}\int_{-\infty}^{t} \mathrm{d}t' \exp(\varepsilon(t-t')) \exp\left(\frac{\mathrm{i}}{\hbar} H(t'-t)\right)$$
$$\times \left(\frac{\partial}{\partial t'}\rho_{rel}(t') + \frac{\mathrm{i}}{\hbar}[H, \rho(t')]\right) \exp\left(-\frac{\mathrm{i}}{\hbar} H(t'-t)\right). \tag{5}$$

The non-equilibrium statistical operator $\rho(t)$ is determined by the relevant statistical operator $\rho_{rel}(t)$ which is a function of the mean values $\langle B_\nu\rangle^{t'}$ at previous time instants $t' < t$. This non-locality in time is usually interpreted as a memory effect. The generalized Kubo approach for the non-equilibrium statistical operator (4), (5) can be employed for the derivation of quantum kinetic equations for, for example, the one-particle distribution function, by taking the operators of single-particle states as the relevant ones [21].

On the other hand, linearizing the general solution (5) with respect to the external field H_F as well as to the response parameters F_ν, and supposing the stationary case $\langle \dot{B}_\nu \rangle = 0$, a generalized Boltzmann equation can be derived [22]:

$$E((\dot{R}, B_\nu) + \langle \dot{R}(\varepsilon); \dot{B}_\nu \rangle) = \sum_{\nu'} F_{\nu'}((\dot{B}_{\nu'}, B_\nu) + \langle \dot{B}_{\nu'}(\varepsilon); \dot{B}_\nu \rangle). \tag{6}$$

The equilibrium correlation functions in equation (6) are defined by

$$(A, B) = \frac{1}{\beta}\int_0^\beta d\tau \, \mathrm{Tr}(\rho_0 A(-i\hbar\tau)B) \qquad A(t) = \exp(iH_S t/\hbar)A(0)\exp(-iH_S t/\hbar)$$
$$\langle A(\varepsilon); B\rangle = \int_{-\infty}^0 dt \exp(\varepsilon t)(A(t), B) \qquad \rho_0 = \frac{1}{Z_0}\exp[-\beta(H_S - uN)]. \tag{7}$$

In this paper, we employ generalized momenta P_n for the set of relevant observables, i.e.

$$\{B_\nu\} \equiv \{P_n\} \qquad P_n = \sum_k \hbar k[\beta E_e(k)]^n a_e^+(k)a_e(k) \qquad \dot{R} = -eP_0/m_e. \tag{8}$$

The most simple contributions P_0 and P_1 determine the electrical and the heat current in the system via

$$\langle j_{el}\rangle = (e/\Omega_0 m_e)\,\mathrm{Tr}\{\rho_{rel}P_0\} \equiv \sigma E \tag{9a}$$
$$\langle j_Q\rangle = (1/\Omega_0 m_e)\,\mathrm{Tr}\{\rho_{rel}(k_B T P_1 - hP_0\}. \tag{9b}$$

(See, e.g., [7].) Ω_0 and h are the system volume and the enthalpy per particle, respectively. Applying a finite set of momenta $P_n (n = 0, 1, \ldots, L)$ for the characterization of the non-equilibrium state, the response parameters F_n have to be determined from equation (6) by Cramer's rule and for the electrical conductivity, σ follows from equation (9*a*) (for details see [7–9]):

$$\sigma = \frac{\beta}{\Omega_0}\begin{vmatrix} 0 & N_0 \\ M_0 & \mathbf{D} \end{vmatrix} \Big/ |\mathbf{D}| \tag{10a}$$

$$N_0 = (N_{00}, N_{01}, \ldots, N_{0L}) \qquad \mathbf{D} = \begin{pmatrix} d_{00} & d_{01} & \ldots & d_{0L} \\ d_{10} & d_{11} & \ldots & d_{1L} \\ \cdot & \cdot & \ldots & \cdot \\ d_{L0} & d_{L1} & \ldots & d_{LL} \end{pmatrix} \qquad M_0 = \begin{pmatrix} N_{00} \\ N_{10} \\ \cdot \\ N_{L0} \end{pmatrix}. \tag{10b}$$

The elements of the determinants are equilibrium correlation functions $N_{0m} = N_{m0} = (P_0, P_m)/m_e$ and $d_{nm} = \langle \dot{P}_n(\varepsilon); \dot{P}_m\rangle$ defined according to (7).

Equation (10) is valid for arbitrary degeneracy. For the non-degenerate case, the Spitzer result for fully ionized plasmas can be obtained within at least a four-momenta approximation (i.e. considering $L = 3$), expressing, furthermore, the correlation functions by T matrices for electron–ion and electron–electron scattering, and calculating these quantities within the partial wave method [6, 10]:

$$\sigma_{Sp} = 0.591[(4\pi\varepsilon_0)^2/e^2 m_e^{1/2}\beta^{3/2}][\ln(3R_D/l)]^{-1} \tag{11}$$

where $l = e^2/(4\pi\varepsilon_0 k_B T)$ is the Landau length, $R_D = [k_B T\varepsilon_0/(2n_e e^2)]^{1/2}$ is the Debye

screening length, and $n_e = N_e/\Omega_0$. For the more general case of dense plasmas, many-particle effects can be treated within the present correlation function method. The influence of dynamic screening [23], Pauli blocking [24], the Debye–Onsager relaxation effect [9], the formation of bound states [7, 11–13] and structure factor effects [6] were investigated for dense hydrogen and alkali plasmas.

For the opposite case, such as that of the degenerate electron systems such as liquid metals which are characterized by a strongly coupled ion system, equation (10) yields, within a one-momentum approximation (i.e. considering only P_0), the well-known Ziman formula

$$\sigma_{Zi}^{-1} = \frac{\Omega_0 m_e^2 N}{12\pi^3\hbar^3 e^2 n_e^2} \int_0^\infty dQ\, Q^3 f(Q/2)\, S(Q) \left| \frac{V_{ei}(Q)}{\varepsilon(Q)} \right|^2 \tag{12}$$

with the ion structure factor

$$S(Q) = \frac{1}{N} \langle \sum_{i,j} \exp[i\, \boldsymbol{Q} \cdot (\boldsymbol{R}_i - \boldsymbol{R}_j)] \rangle$$

the dielectric function $\varepsilon(Q)$ and the Fermi distribution function $f(E) = [\exp(\beta(E - \mu_e)) + 1]^{-1}$. The usual Ziman formula describes the resistivity of a liquid metal on the basis of the nearly free electron model, it depends on the appropriate choice of the electron–ion pseudopotential $V_{ei}(Q)$ and the approximation for the dielectric function $\varepsilon(Q)$.

Winter *et al* [2, 3] observed a deviation of the electrical conductivity from the Ziman formula (12) at densities approaching the critical density when applying the measured data for the static structure factor $S(Q)$ of caesium. The present approach (10) allows for different improvements of the usual Ziman formula which can be considered for the explanation of these observed deviations:

(i) allowance for arbitrary degeneracy,

(ii) inclusion of higher momenta P_n for the calculation of the electrical conductivity (10),

(iii) consideration of electron–electron scattering processes,

(iv) treatment of the ionization equilibrium which accounts for bound electrons and which leads to a decrease of the number of free charge carriers.

Furthermore, we investigate the influence on the numerical results for the electrical conductivity of different pseudopotentials $V_{ei}(Q)$ (Ashcroft empty-core potential [25], the Heine–Abarenkov potential [26], and a modified version of Hasegawa *et al* [27]) and different screening functions $\varepsilon(Q)$ (Lindhard function with local-field corrections).

We have to calculate the equilibrium correlation functions N_{0m}, d_{nm} in order to determine the electrical conductivity (10*a*). The generalized particle numbers N_{0m} are given by

$$N_{0m} = N_e[\Gamma(m + 5/2)/\Gamma(5/2)][I_{m+1/2}(\alpha_e)/I_{1/2}(\alpha_e)] \tag{13}$$

where $I_n(x)$ denotes Fermi integrals and $I_{1/2}(\alpha_e) = n_e\lambda_e^3/2$, $\lambda_e^2 = 2\pi\beta\hbar^2/m_e$ being the electronic thermal wave length. The force–force correlation functions d_{nm} can be decomposed into the relevant scattering contributions of the free (conducting) electrons, i.e. electron–ion and electron–electron scattering processes:

$$d_{nm} = d_{nm}^{ei} + d_{nm}^{ee}$$

$$d_{nm}^{ei} = \frac{\Omega_0^2 m_e^2 N}{12\pi^3\hbar^3} \int_0^\infty dk \left(-\frac{df(k)}{dk} \right) \left(\frac{\beta\hbar^2 k^2}{2m_e} \right)^{n+m} L(k) \tag{14a}$$

$$L(k) = \int_0^{2k} \mathrm{d}Q\, Q^3\, S(Q) \left| \frac{V_{ei}(Q)}{\varepsilon(Q)} \right|^2$$

$$d_{11}^{ee} = \frac{m_e^{5/2}\Omega_0}{\beta^{1/2}\hbar^4 2^7 \pi^6} \int_0^\infty \mathrm{d}s\, s^2 \int_0^\infty \mathrm{d}p\, p \int_0^\infty \mathrm{d}Q\, Q^3 \int_{-1}^{1} \mathrm{d}x \left| \frac{V_{ee}(Q)}{\varepsilon(Q)} \right|^2$$
$$\times \{\tfrac{1}{4}(p^2 - s^2)^2 + s^2x^2(s^2 + p^2 - 2s^2x^2)\}$$
$$\times [A + 1/A + 2\cosh(sQx/2)]^{-1}\, [B + 1/B + 2\cosh(pQx/2)]^{-1} \qquad (14b)$$

$$A = \exp(s^2/2 + Q^2/8 - \beta\mu_e) \qquad B = \exp(p^2/2 + Q^2/8 - \beta\mu_e) \qquad d_{0m}^{ee} = d_{m0}^{ee} = 0.$$

The electron–ion contribution was determined by means of the Ashcroft empty-core potential $V_{ei}^{A}(Q)$, the Heine–Abarenkov potential $V_{ei}^{HA}(Q)$, and a new local empty-core potential $V_{ei}^{H}(Q)$ proposed recently by Hasegawa *et al* [27]:

$$V_{ei}^{A}(Q) = [-4\pi Ze^2/Q^2]\cos(QR_C) \qquad V_{ei}^{HA}(Q) = [-4\pi Ze^2/(Q^3R_C)]\sin(QR_C)$$
$$V_{ei}^{H}(Q) = [-4\pi Ze^2/Q^2]\cos(Qr_C)[[1 + aQ^2/(Q^2 + b^2)]\exp(-bR_C)(1 + \tan(Qr_C))]. \qquad (15)$$

The respective cut-off radii R_C were chosen to match the electrical conductivity near the melting point, measured by Cook [28]. The values of a and b are due to Matsuda *et al* [29] who determined the parameters $a = 22$ and $b = 1.2/a_B$ (a_B Bohr radius) so as to fit the form of the pseudopotential to the electron–ion potential which was calculated in the local density functional approximation. However, they have chosen the cut-off radius $R_C = 3.25\, a_B$ so as to reproduce theoretically the position of the first peak and the low-Q behaviour of the observed structure factor $S(Q)$ near the triple point.

The dielectric function can be represented as

$$\varepsilon(Q) = 1 + [1 - G(Q)]g_H 4\pi e^2/Q^2$$
$$g_H = (k_F m_e/\pi^2\hbar^2)[\tfrac{1}{2} + (4k_F^2 - Q^2/4k_F Q)\ln|(2k_F + Q)/(2k_F - Q)|] \qquad (16)$$

where g_H denotes the Hartree screening function which is decreased due to local-field corrections $G(Q)$. The influence of different expressions for $G(Q)$ is investigated. We apply here the expressions derived by Sham [30], Shaw [31], and Ichimaru and Utsumi [32] (see also Vashishta and Singwi [33]).

The static structure factor $S(Q)$ which enters into the Coulomb logarithm $L(k)$ was taken from experiment [2]. The electron–electron contribution to the correlation function was calculated numerically for arbitrary degeneracy [34], it tends to lower the electrical conductivity. $V_{ee}(Q) = 4\pi e^2/Q^2$ denotes the Coulomb potential.

3. Comparison of experimental and theoretical results for the electrical conductivity

We have considered the following improvements in order to explain the deviations observed in the experimental values for the DC conductivity when compared with a calculation using the simple Ziman formula.

3.1. Arbitrary degeneracy

The replacement of the sharp Fermi surface (integration $\int_0^{2k_F} dQ \ldots$) for complete degeneracy by the Fermi distribution function (integration $\int_0^\infty dQ f(Q/2) \ldots$) for arbitrary degeneracy has only a small effect on the results, because the electron system is still in the degenerate domain above the critical density considered here. However, for lower densities characteristic of the vapour phase, these effects become important. For instance, the electrical conductivity is increased by about 8% for the lowest density given here.

3.2. Inclusion of higher momenta

The Zubarev method for calculating the electrical conductivity (10*a*) is rapidly converging with respect to a systematic extension of the set of relevant momenta $\{P_n\}$ [10, 13, 34]. For instance, the Spitzer result (11) valid for the low-density limit is obtained within even a four-momenta approximation. With increasing density, the influence of higher momenta becomes less important and in the limit of complete degeneracy a one-momentum approximation yields the Ziman formula (12) [35]. For the nearly critical region considered here, the degeneracy of the electron system is not complete and the consideration of higher momenta P_n for calculating the electrical conductivity (10*a*) leads to an increase of the respective values. However, the increase within a three-momenta approximation amounts to less than 1% for the densities considered here.

3.3. Electron–electron scattering

When including higher momenta, we have to consider, in addition, the electron–electron correlation functions d_{nm}^{ee} ($d_{00}^{ee} = 0$). Electron–electron scattering leads to a lowering of the electrical conductivity. In the low-density limit (11), the prefactor of the conductivity is therefore 0.591 instead of 1.015 for a Lorentz gas. The influence of electron–electron scattering decreases with increasing density (compare [34]) and vanishes in the limit of complete degeneracy. For the conditions considered here, electron–electron scattering decreases the electrical conductivity by up to 10% for the lowest density of about 1×10^{21} cm^{-3}.

Before we present the results accounting for partial ionization, the influence of the chosen electron–ion pseudopotential and of the screening function are discussed. We have calculated the electrical conductivity (10*a*), (14) within a one-momentum approximation applying the Ashcroft, Heine–Abarenkov and Hasegawa pseudopotentials and inserting in all cases different expressions for the local-field corrections in the dielectric function [30–32], see table 1. The choice of the electron–ion pseudopotential affects the results for the electrical conductivity only weakly. The use of the Hasegawa empty-core potential gives rise to small improvements as compared with the Ashcroft potential. However, local-field corrections have a strong influence on the results and the best data currently available, Ichimaru and Utsumi [32], yield a lowering of the electrical conductivity of about 50% in comparison to the values observed with the Sham dielectric function [30] for the lowest densities considered here. Both the Ashcroft and the Heine–Abarenkov potentials yield conductivities lower than the experimental values for densities greater than about 1.3 g cm^{-3}. The last row in table 1, the Hasegawa empty-core potential with local-field corrections in the Ichimaru and Utsumi [32] form, shows the best overall agreement.

Table 1. The electrical conductivity (12) of Cs liquid in $\Omega^{-1}\,cm^{-1}$ using various pseudopotentials $V(Q)$ and local field corrections in the dielectric function $\varepsilon(Q)$ for different temperatures T and densities ρ. The cut-off radii R_C were fitted to match the measured electrical conductivity [28] for $T = 373$ K and $\rho = 1.8\,g\,cm^{-3}$.

T (K) / ρ (g cm^{-3})	$V(Q)$	Ashcroft			Heine–Abarenkov			Hasegawa		
	$\varepsilon(Q)$	Sham	Shaw	IU	Sham	Shaw	IU	Sham	Shaw	IU
373										
1.800		22160	22140	22180	22190	22210	22190	22240	22010	22190
773										
1.567		10240	9196	8890	10670	9244	8999	9992	10470	10810
973										
1.452		8237	7095	6681	8669	7189	6845	7978	8224	8329
1173										
1.332		6123	4880	4560	6502	5030	4767	5894	5618	5618
1373										
1.209		5140	3830	3567	5481	3998	3783	4936	4342	4297
1673										
0.956		2936	1916	1731	3151	2040	1877	2808	2119	2003
1923										
0.590		1488	815	701	1592	875	767	1430	868	767
R_c (a_B)		2.214	2.516	2.502	4.125	4.685	4.683	2.576	2.851	2.855

In table 2 we compare these values ('B') with the experimental data of Cook [28] and Noll *et al* [4]. For comparison we present the results of the most simple approach using the Ziman formula (sharp Fermi surface) with the Ashcroft potential and the local-field corrections by Sham. Furthermore, we present the electrical conductivity given by Hoshino *et al* [36] ('A') which was obtained by means of the Ziman formula (12) with the Hasegawa potential and with local field corrections by Ichimaru and Utsumi (with the cut-off radius R_C fitted by Matsuda *et al* [29] to the observed structure data). The deviation of our numerical results from the experimental data is less than 10% for densities up to $1.3\,g\,cm^{-3}$. For lower densities the theoretical results are still up to 50% too high. For conditions less than about three times the critical density another mechanism obviously becomes operative, which leads to a further lowering of the electrical conductivity.

3.4. Ionization equilibrium

The analysis of the equation of state data within a model calculation for the composition of dense alkali plasmas [11] indicates that the degree of ionization is strongly reduced near the critical point due to the formation of bound states (localized electrons). Besides atoms Cs, also dimers Cs_2 and molecular ions Cs_2^+ are formed. They can reach a maximum concentration of about 20% and 40%, respectively, near the critical point (see figure 2). This is in good agreement with the results obtained by measurements of

Table 2. The electrical conductivity of Cs liquid in $\Omega^{-1}\,cm^{-1}$ obtained from equation (12) compared to the experimental values of Cook [28] and Noll *et al* [4]. Ashcroft and Sham: Ashcroft empty-core potential and Sham dielectric function [30]; Hasegawa and IU: Hasegawa empty-core potential and Ichimaru/Utsumi dielectric function [32]. A, results of Hoshino *et al* [36] with R_C fitted to observed structure data; B, present calculation with R_C fitted to the conductivity at the melting point; C, consideration of the ionization equilibrium (the degree of ionization is given in the brackets).

		Hasegawa and IU			
T (K) ρ (g cm^{-3})	Ashcroft and Sham	A	B	C (α_{ion})	Experiment
373 1.800	22200	16600	22000		22196 [28]
773 1.567	10100	14100	10800		10200 [4]
973 1.452	8060	12900	8330	8330 (1.00)	7800 [4]
1173 1.332	5940	10000	5620	5040 (0.95)	5070 [4]
1373 1.209	4940	7080	4300	3840 (0.94)	3550 [4]
1673 0.956	2760	3090	2000	1670 (0.90)	1770 [4]
1923 0.590	1370	490	770	460 (0.70)	500 [4]
R_c (a_B)	2.214	3.25		2.855	

the magnetic susceptibility [37]. The extension of the present theoretical approach (10) to the more general case of partial ionization can immediately be performed [7, 11–13]. The strong decrease of the electrical conductivity near the critical point can be explained by the reduction of the number of charge carriers due to the formation of bound states.

The ionization equilibrium becomes effective for densities below $\rho = 1.3\ g\ cm^{-3}$. The number of free charge carriers, and thus also the electrical conductivity, decreases on approaching the critical point. The respective values for σ are indicated in table 2 by the label 'C' and show a better agreement with the experimental values for nearly critical conditions. The degree of ionization resulting from the calculation of the equation of state for alkali plasmas [11] is given in the brackets.

4. Conclusions

The deviations from the usual Ziman formula at densities below 1.3 g cm^3 occur in that range where the onset of the magnetic susceptibility enhancement [37, 38] and the

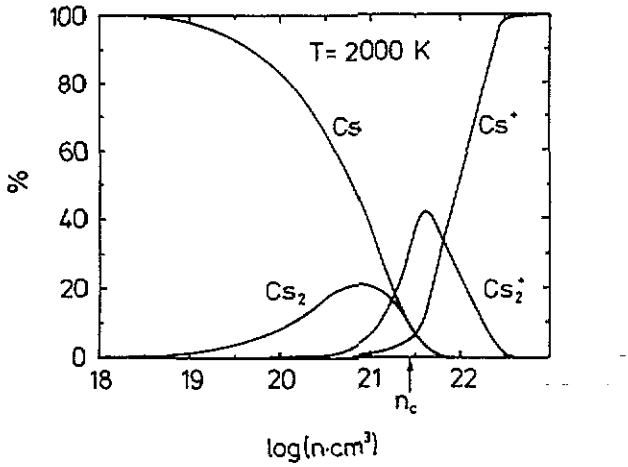

Figure 2. The composition of caesium for $T = 2000$ K as a function of the total ion density [11].

increase of the effective electron mass as obtained from optical measurements [39] indicated that electron–electron correlation becomes important. Though its effect on the electrical conductivity is small in this density region, our calculations have also shown that electron–electron scattering is not negligible.

The influence of smeared-out Fermi surface and of higher momenta in calculating the electrical conductivity is small in the parameter region considered here.

We have shown that the empty-core potential of Hasegawa *et al* [27] gives rise to slightly improved results for the electrical conductivity compared with the use of the Ashcroft and the Heine–Abarenkov potential. The consideration of local-field corrections in the dielectric function decreases the screening effects of the electron–ion interaction and thus, also, the electrical conductivity compared with the case of only Hartree screening. In particular, considering local-field corrections in the Ichimaru and Utsumi [32] form yields a reasonable agreement with experimental data [4] except for nearly critical conditions.

The main effect in the drastic lowering of the electrical conductivity below 1.3 g cm^{-3} as it was experimentally observed, and could not be described by any systematic improvement of the Ziman formula (12), seems to be the reduction of the number of free charge carriers due to the formation of bound states.

References

[1] Hensel F and Uchtmann H 1989 *Ann. Rev. Phys. Chem.* **40** 61
[2] Winter R, Hensel F, Bodensteiner T and Gläser W 1987 *Ber. Bunsenges. Phys. Chem.* **91** 1327
[3] Winter R and Hensel F 1989 *Phys. Chem. Liq.* **20** 1
[4] Noll F, Pilgrim W-C and Winter R 1988 *Z. Phys. Chem., NF* **156** 303
[5] Jüngst S, Knuth B and Hensel F 1985 *Phys. Rev. Lett.* **55** 2160
[6] Meister C-V and Röpke G 1982 *Ann. Phys., Lpz.* **39** 133
[7] Höhne F E, Redmer R, Röpke G and Wegener H 1984 *Physica* A **128** 643
[8] Christoph V and Röpke G 1985 *Phys. Status Solidi* b **131** 11
[9] Röpke G 1988 *Phys. Rev.* A **38** 3001

[10] Sigeneger F, Arndt S, Redmer R, Luft M, Tamme D, Kraeft W D, Röpke G and Meyer T 1988 *Physica* A **152** 365
[11] Redmer R and Röpke G 1989 *Contr. Plasma Phys.* **29** 343
[12] Bialas F, Schlanges M, Redmer R and Schmidt K 1989 *Contr. Plasma Phys.* **29** 413
[13] Reinholz H, Redmer R and Tamme D 1989 *Contr. Plasma Phys.* **29** 395
[14] Spitzer L and Härm R 1953 *Phys. Rev.* **69** 977
[15] Ziman J M 1961 *Phil. Mag.* **6** 1013
[16] Zubarev D N 1974 *Nonequilibrium Statistical Thermodynamics* (New York: Plenum)
[17] Zwanzig R 1960 *J. Chem. Phys.* **33** 1338
Nakajima S 1958 *Prog. Theor. Phys.* **20** 948
[18] Robertson B 1966 *Phys. Rev.* **144** 151
[19] Bogolyubov N N 1946 *Problems of Dynamical Theory in Statistical Physics* (Moscow: Gostekhizdat) (in Russian)
[20] Zubarev D N 1970 *Itogi Nauki i Tekhniki* vol 15 (Moscow) p 131
[21] Röpke G and Schulz H 1988 *Nucl. Phys.* A **477** 472
[22] Röpke G 1983 *Physica* A **121** 92
[23] Redmer R, Röpke G, Morales F and Kilimann K 1990 *Phys. Fluids B: Plasma Physics* **2** 390
[24] Schmidt M, Janke T and Redmer R 1989 *Contr. Plasma Phys.* **29** 431
[25] Ashcroft N W 1968 *Proc. Phys. Soc.* **1** 232
[26] Heine V and Abarenkov I 1964 *Phil. Mag.* **9** 451
[27] Hasegawa M, Hoshino K, Watabe M and Young W H 1990 *J. Non-Cryst. Solids* **177** & **118** 300
[28] Cook J G 1982 *Can. J. Phys.* **60** 1759
[29] Matsuda N, Mori H, Hoshino K and Watabe M 1991 *J. Phys. Soc. Japan* at press
[30] Sham J 1965 *Proc. R. Soc. (Series A)* **283** 33
[31] Shaw R W 1970 *J. Phys. C: Solid State Phys.* **3** 1140
[32] Ichimaru S and Utsumi K 1981 *Phys. Rev.* B **24** 7385
[33] Vashishta P and Singwi K S 1972 *Phys. Rev.* B **6** 875
[34] Röpke G and Höhne F E 1981 *Phys. Status Solidi* b **107** 603
[35] Reinholz H 1989 *PhD thesis* Rostock
[36] Hoshino K, Matsuda N and Watabe M 1991 *J. Phys. Soc. Japan* at press
[37] Freyland W 1979 *Phys. Rev.* B **20** 5104
[38] Warren Jr. W W, Brennert G F and El-Hanany U 1989 *Phys. Rev.* B **39** 4038
[39] Knuth B 1990 *PhD thesis* Marburg